Acta Crystallographica Section D
**Biological Crystallography**
ISSN 0907-4449

# Determination by MAD-DM of the structure of the DNA duplex d[ACGTACG(5-BrU)]$_2$ at 1.46 Å and 100 K

**Alan K. Todd,[a] Adrienne Adams,[b] Harold R. Powell,[c] Deborah J. Wilcock,[a] James H. Thorpe,[a] Andrea Lausi,[d] Franco Zanini,[d] Laurence P. G. Wakelin[e] and Christine J. Cardin[a]***

[a]Department of Chemistry, The University of Reading, Whiteknights, Reading RG6 6AD, England, [b]Department of Biochemistry, Trinity College, Dublin 2, Ireland, [c]The Chemical Laboratory, Lensfield Road, Cambridge CB2 1EW, England, [d]Sincrotrone Elettra, Padriciano, Trieste, 99-I-34012, Italy, and [e]Cancer Drug Discovery, Department of Chemistry, University College Dublin, Belfield, Dublin 4, Ireland

Correspondence e-mail: c.j.cardin@reading.ac.uk



Received 15 July 1998
Accepted 30 September 1998

**NDB Reference:** d[ACGTACG(5-BrU)]$_2$, ADHB99.

A four-wavelength MAD experiment on a new brominated octanucleotide is reported here. d[ACGTACG(5-BrU)], $C_{77}H_{81}BrN_{30}O_{32}P_7$, $M_r$ (DNA) = 2235, tetragonal, $P4_32_12$ (No. 96), $a$ = 43.597, $c$ = 26.268 Å, $V$ = 49927.5 Å$^3$, $Z$ = 8, $T$ = 100 K, $R$ = 10.91% for 4312 reflections between 15.0 and 1.46 Å resolution. The self-complementary brominated octanucleotide d[ACGTACG(5-BrU)]$_2$ has been crystallized and data measured to 1.45 Å at both 293 K and a second crystal flash frozen at 100 K. The latter data collection was carried out to the same resolution at the four wavelengths 0.9344, 0.9216, 0.9208 and 0.9003 Å, around the Br $K$ edge at 0.92 Å and the structure determined from a map derived from a MAD data analysis using pseudo-MIR methodology, as implemented in the program *MLPHARE*. This is one of the first successful MAD phasing experiments carried out at Sincrotrone Elettra in Trieste, Italy. The structure was refined using the data measured at 0.9003 Å, anisotropic temperature factors and the restrained least-squares refinement implemented in the program *SHELX*96, and the helical parameters are compared with those previously determined for the isomorphous d(ACGTACGT)$_2$ analogue. The asymmetric unit consists of a single strand of octamer with 96 water molecules. No countercations were located. The A-DNA helix geometry obtained has been analysed using the *CURVES* program.

## 1. Introduction

Multiwavelength anomalous diffraction methodology (see *e.g.* Hendrickson, 1991; Hendrickson & Ogata, 1997) has grown rapidly in popularity during the last couple of years (see *e.g.* Powell, 1997; Crane *et al.*, 1997), thanks to the availability of readily tunable synchrotron sources (Smith, 1997). The present investigation was prompted by our desire to solve the structures of a number of drug–DNA complexes for which the molecular-replacement method using *AMoRe* had been completely unsuccessful and for which there had been many problems preparing isomorphous derivatives using brominated oligonucleotides. Molecular-replacement methodology is frequently unsuccessful for DNA duplex structures. Among the possible rationales for this observation are difficulty in separating inter- and intramolecular Patterson vectors when the molecule is a long cylinder, and is closely packed in certain directions. Additionally, the polymorphism of DNA conformations means that in practice there is a wide range of backbone positions (note the conclusions in the present work about the effect of bromination on groove width). A detailed discussion of these problems and their possible solution has recently been published (Baikalov & Dickerson, 1998).

Since carrying out the present work, we have used the essentially identical methodology, only lacking the high-

energy offset data, to solve the first oligonucleotide structure containing an acridine-4-carboxamide derivative (Todd *et al.*, 1999), and in that case the main packing force is undoubtedly stacking interactions and the resulting structure quasi-polymeric. The success of the experiment reported here gave us the confidence to use the same technique in a case where other methods of structure solution had been unproductive.

The MAD method relies for its success on the careful measurement of anomalous differences (Peterson *et al.*, 1996) and its success is highly dependent on the characteristics of the source. The third-generation source at Elettra, Trieste, Italy, has a stable, intense beam, and data collected there yielded MAD phases which, in combination with density modification and histogram matching, yielding a very clear electron-density map by the methods described here. Given the availability of a suitable synchrotron source, the combination of cryocooling and multiwavelength measurements around the Br *K* edge at 0.92 Å can, therefore, be a successful strategy for solving new DNA structures. The present paper reports our initial trial of this procedure using the brominated analogue of the octamer $d(ACGTACGT)_2$, which we previously studied using only a sealed tube molybdenum source (Wilcock *et al.*, 1996). We have also (not reported here) carried out a refinement of that sequence to 1.45 Å against data collected at room temperature, with essentially identical results.

## 2. Experimental

The oligodeoxyribonucleotide of sequence ACGTACG(5-BrU) was synthesized by solid-phase methods on an Applied Biosystems DNA synthesizer using phosphoramidite chemistry, and purified using ion-exchange and reverse-phase high-pressure liquid chromatography. Crystals were grown at 285 K by vapour diffusion using the sitting-drop technique. A 10 µl drop containing 0.5 m*M* DNA, 50 m*M* cacodylate buffer, pH 6.5, 2.0 m*M* magnesium acetate, 3.0 m*M* spermine–4HCl and 5% 2-methyl-2,4-pentanediol was equilibrated against a 1 ml reservoir containing 30% MPD. Microcrystals formed within one week but over a period of a further 12 weeks these redissolved and tetragonal bipyramids grew which were suitable for X-ray analysis.

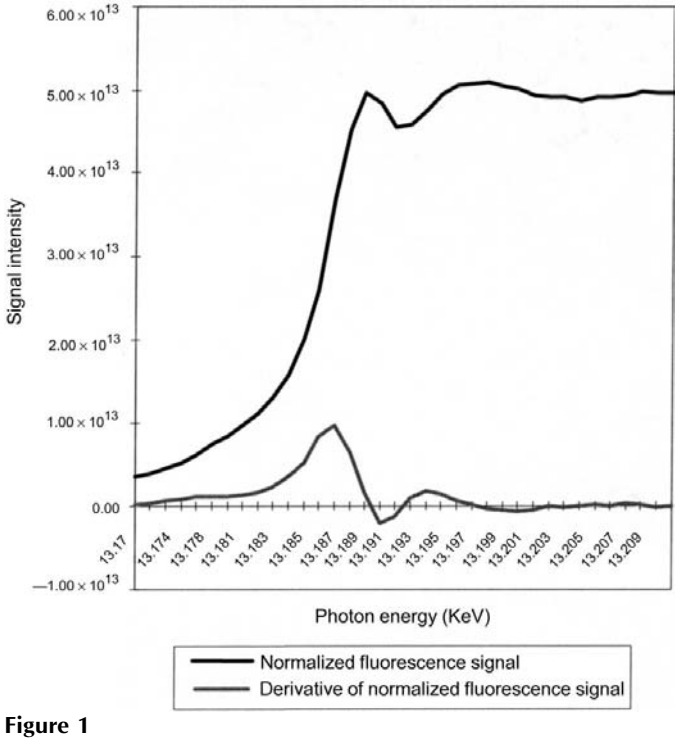


**Figure 1**
The fluorescence spectrum of 5-bromouridine, measured just before the experiment.

**Table 1**
Summary of data-collection statistics.

The crystal is tetragonal $P4_32_12$ (No. 96), $a$ = 43.597, $c$ = 26.268 Å, $V$ = 49927.5 Å$^3$, $Z$ = 8, $T$ = 100 K. The crystal-to-detector distance was 120 mm and data were collected to a resolution of about 1.4 Å (this of course varies slightly with the wavelength for a fixed geometry), with an average exposure time of 15 min.

| | $\lambda_1$ | $\lambda_2$ | $\lambda_3$ | $\lambda_4$ |
|---|---|---|---|---|
| Wavelength (Å) | 0.9344 | 0.9216 | 0.9208 | 0.9003 |
| Total data | 12171 | 25725 | 26727 | 28390 |
| Unique data | 4276 | 5672 | 5867 | 6301 |
| Linear *R* factor | 0.051 | 0.071 | 0.058 | 0.061 |
| Square *R* factor | 0.074 | 0.105 | 0.100 | 0.096 |
| Completeness | 74.3 | 98.7 | 98.6 | 98.3 |
| No. of frames | 15 | 30 | 30 | 30 |

A crystal of the DNA octanucleotide duplex $d[ACGTACG(5\text{-}BrU)]_2$ with approximate dimensions 0.6 × 0.3 × 0.25 mm was mounted in a loop coated with Riedel-de Haen perfluoropolyether RS3000 oil, and flash frozen at 100 K on the X-ray diffraction beamline at Sincrotrone Elettra, Trieste. Data were collected on a MAR Research 18 cm image plate as in Table 1, at four wavelengths around the Br edge at 0.92 Å. The crystal was approximately aligned along one of the non-unique tetragonal axes, thus recording many Bijvoet pairs close together in time. Subsequent data processing showed that crystal decay was negligible, so this factor may not have been significant in this experiment. Data were collected to a resolution of 1.4 Å, and 30 frames of data, each of 3° rotation, were collected for each wavelength, starting with the inflection point. For the last wavelength (the low-energy offset) only 15 frames of data could be measured. The inflection point data set was subsequently treated as the 'native' data set when using *MLPHARE*. The fluorescence spectrum for the Br edge was measured before the experiment using a sample of 5-bromouridine (Fig. 1) and subsequent analysis showed that we had determined the position of this inflection point with sufficient precision to generate useful phase information. The chemical environment of the Br atom in 5-bromouridine is sufficiently similar to that in the octamer to introduce negligible shift of the absorption edge. This is an apparently more favourable situation than with proteins, where the shift on incorporation of the anomalous scatterer into the protein is normally assumed to be not negligible.

### 2.1. Scaling and merging of data

Data processing was carried out using *DENZO* (Otwinowski, 1993), giving the statistics in Table 1. Once the data was

**Table 2**
Scaling statistics for the four data collections.

$n_{refs}$, number of reflections; $N$ (an), number of reflections with anomalous difference; mean (an), mean anomalous difference; mean (|an|), mean absolute anomalous difference; max (an), maximum anomalous difference; $K_{emp}$, mean dispersive difference/(0.5 mean anomalous difference).

| | $N_{refs}$ | Scale | $r_{fac}$ | $N$ (an) | Mean (an) | Mean (\|an\|) | Max (an) | $K_{emp}$ |
|---|---|---|---|---|---|---|---|---|
| 1–2 | 2699 | 1.007 | 0.057 | 1557 | 0.5 | 4.8 | 38 | 3.1322 |
| 2–2 | 3226 | — | — | 2426 | 0.2 | 7.3 | 86 | — |
| 2–3 | 3219 | 1.003 | 0.036 | 2424 | 0.1 | 13.0 | 58 | 0.7289 |
| 2–4 | 3209 | 0.999 | 0.051 | 2421 | 0.1 | 10.1 | 54 | 1.33 |

**Table 3**
Data used in determination of heavy-atom positions.

| | | *x/a* | *y/b* | *z/c* | |
|---|---|---|---|---|---|
| $\lambda_3$ | Anomalous white line | 0.9494 | 0.3896 | −0.0036 | cfom 0.014 |
| $\lambda_4$ | Short wavelength offset | 0.5502 | 0.1102 | −0.0042 | cfom 0.019 |

**Table 4**
Data for the three 'derivatives'.

| Derivative | 1($\lambda_1$) | 2($\lambda_3$) | 3($\lambda_4$) |
|---|---|---|---|
| Number of centric reflections | 449 | 768 | 761 |
| Phase difference | 74.3 | 80.4 | 79.7 |
| SD of phase difference | 88.6 | 89.5 | 89.4 |
| Isomorphous difference | 11.0 | 7.1 | 10.2 |
| Lack of closure | 10.0 | 5.3 | 7.6 |
| Phasing power | 0.52 | 0.91 | 1.00 |
| Cullis *R* | 0.91 | 0.75 | 0.75 |

processed it was scaled together using *SCALEPACK*, keeping Bijvoets ($I^+$ and $I^-$) separate both in scaling and the output file. Programs from the *CCP*4 suite (Collaborative Computational Project, Number 4, 1994) were then used as follows. Each file was converted into MTZ format with *F2MTZ*. *TRUNCATE* was then applied to calculate the best estimate of $F$ from $I$. A complete list of reflections between the resolution limits of the data was produced using *UNIQUE*, and this was collected together with the rest of the data in a single file with *CAD*. The data was scaled together using the inflection point data ($\lambda_2$) as the 'native' data set with *SCALEIT*. Data to 1.6 Å resolution were used for structure solution. The output from the scaling process is summarized in Table 2, the scaling factors showing the negligible crystal decay, and significant information content in both anomalous and dispersive differences.

### 2.2. Determination of heavy-atom positions

The Br-atom location can be determined from either the anomalous or the dispersive differences using the direct methods or the Patterson routine for $\Delta F$ data in *SHELXS*96, such as the equivalent correct solutions from the anomalous differences given in Table 3.

The heavy-atom position from $\lambda_3$ was used as the initial heavy-atom position for phase refinement using *MLPHARE*. This was carried out using $\lambda_2$ (inflection point wavelength) as the 'native' data set, in order to take advantage of the largest dispersive difference (*i.e.* between these data and the high-energy offset data). The Br-atom positions and real occupancies of the three 'derivative' data sets were refined, using only centric data. The angle interval for calculation of the phase probability curve was 10° for the eight refinement cycles carried out (Table 4).

The refined Br positions were used to carry out another eight refinement cycles using all data (including the acentric reflections). The real and anomalous occupancies for the three 'derivatives' were refined and the anomalous occupancy for the 'native' was refined while setting its real occupancy to zero. Phased reflections of the inflection point data were output and solvent-flattening and histogram-matching calculations applied with the program *DM* using a solvent content of 0.53. An electron-density map was then calculated from the phased reflections using *FFT*, revealing the clear density shown for the four separate base pairs in Fig. 2.

The density calculated from MAD-DM phases, was superimposed on the model from the native d(ACGT-ACGT)$_2$ structure, previously determined in this laboratory (Wilcock *et al.*,

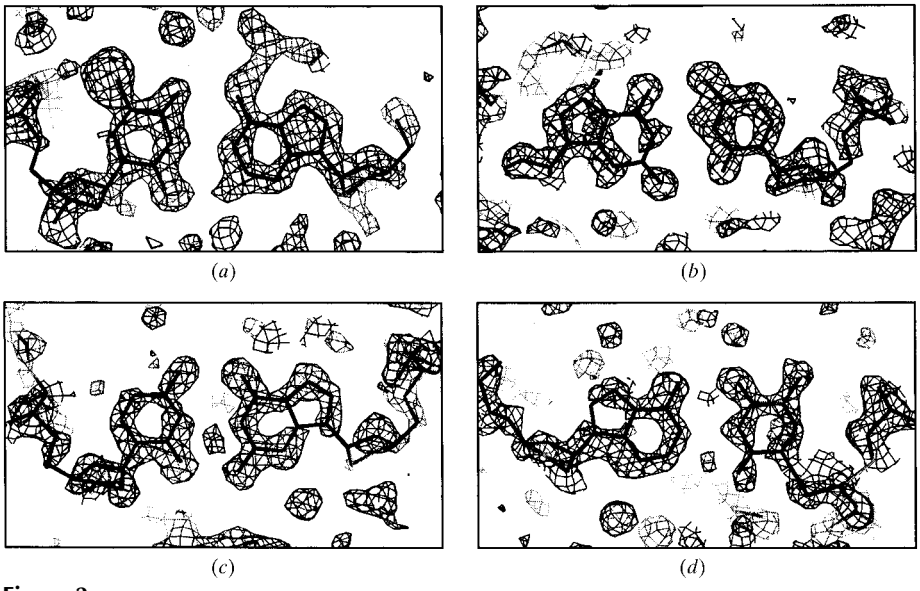


**Figure 2**
Electron density of four base pairs of d[ACGTACG(5-BrU)]$_2$ calculated using MAD-DM phases, superimposed on the model from d(ACGTACGT)$_2$ (Wilcock *et al.*, 1996). Bases are: (*a*) A(1)/5-BrU(16), (*b*) C(2)/G(15), (*c*) G(3)/C(14), (*d*) T(4)/A(13).

**Table 5**
Experimental data for d[ACGTACG(5-BrU)]$_2$.

| | |
|---|---|
| Space group | $P4_32_12$ (No. 96) |
| Cell constants (Å,°) | $a = b = 43.597$ |
| | $c = 26.268$ |
| | $\alpha = \beta = \gamma = 90.00$ |
| Cell volume (Å$^3$) | 49928 |
| Vol/bp (Å$^3$) | 1560 |
| Crystal dimensions (mm) | $0.6 \times 0.3 \times 1.25$ |
| Unique reflections collected | 4555 at 1.46 Å |
| $Z$ | 8 |
| Conventional $R$ factor | 10.91 |
| Temperature (K) | 100 |

1996). Because the model fits the density well, it was used as the starting model for refinement without modification, other than replacing the C5M of the terminal thymine base with Br. The structure was refined, with *SHELXL*, against the highest resolution data set (λ4), using 2738 restraints (Sheldrick & Gould, 1995). 1,2 and 1,3 (bond length and angle) restraints were applied but not 1,4 (torsional) restraints, followed by location of 96 water molecules using the program *SHELXWAT*. This routine appears to be more efficient than hand location of water molecules, but will not locate either $Mg^{2+}$ or spermine countercations. The $F_o - F_c$ map obtained after isotropic refinement by the conjugate-gradient least-squares method before and after water location was carefully examined using the program *O* (Jones *et al.*, 1991) for density which might be atoms other than water (on geometric criteria) but none could be located convincingly. This result parallels the one we obtained previously, when we also could see no convincing density for cations. In the final cycles of refinement anisotropic temperature factors were used for all non-H atoms (using 5% of the data in an $R_{\rm free}$ test to examine whether this was justified, the value of $R_{\rm free}$ was 0.2003 after 20 cycles of conjugate-gradient least squares, (although the data set is really too small for meaningful statistics) with all data being used in the final refinement cycles). The last refinement cycle was full-matrix least squares (2230 parameters, 2730 restraints), and gave a final conventional $R$ factor of 10.91% for 4312 reflections having $F_o > 4\sigma(F_o)$, and 11.15% for all 4555 data.

Two stereo representations of the duplex are shown in Fig. 3. The coordinates and structure factors for this structure have been deposited with the Nucleic Acid Data Bank (accession number ADHB99). Using their checking software, the r.m.s. deviation for covalent bonds relative to the standard dictionary (Clowney *et al.*, 1996; Gelbin *et al.*, 1996) is 0.059 Å, and the r.m.s. deviation for covalent angles relative to the standard dictionary is 2.3°, and there are no incorrect chiral centres.

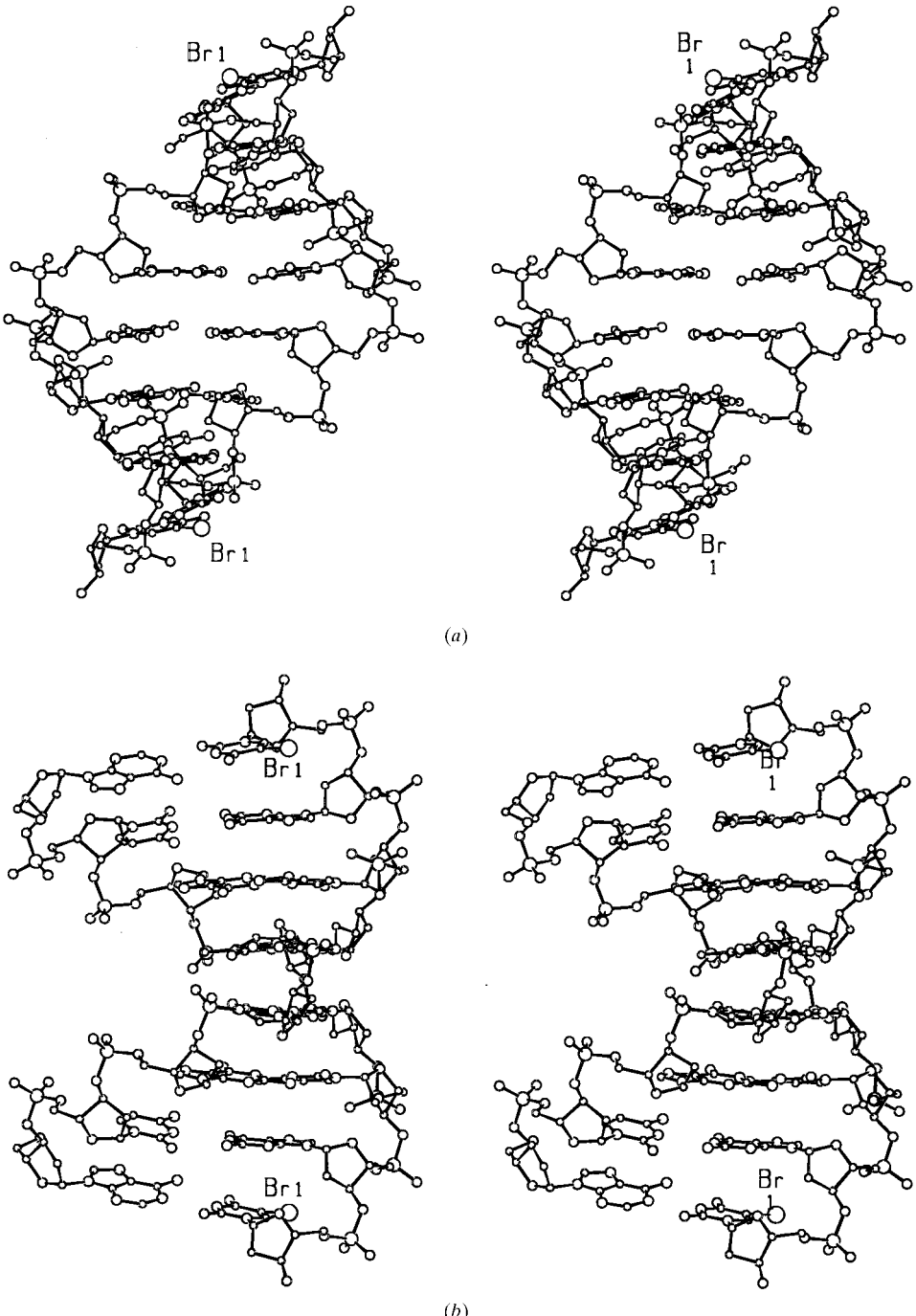


**Figure 3**
(*a*) Stereo pair of the refined duplex looking down the twofold axis and with the helix axis vertical, and (*b*) with the twofold axis horizontal (rotation by 90° viewed from the direction of *a*).

**Table 6**
Backbone torsion angles (°) for d[ACGTACG(5-BrU)] calculated using *CURVES* (Lavery & Sklenar, 1989).

The torsion angles are defined as: $\alpha$ = O3′—P—O5′—C5′, $\beta$ = P—O5′—C5′—C4′, $\gamma$ = O5′—C5′—C4′—C3′, $\delta$ = C5′—C4′—C3′—O3′, $\varepsilon$ = C4′—C3′—O3′—P, $\zeta$ = C3′—O3′—P—O5′, $\chi$ = O4′—C1′—N9—C4 (for purines) or $\chi$ = O4′—C1′—N1—C2 (for pyrimidines).

| Base | $\alpha$ P—O5′ | $\beta$ O5′—C5′ | $\gamma$ C5′—C4′ | $\delta$ C4′—C3′ | $\varepsilon$ C3′—O3′ | $\zeta$ O3′—P | $\chi$ C1′—N |
|---|---|---|---|---|---|---|---|
| A(1) | −72 | 167 | 51 | 81 | −145 | −66 | −163 |
| C(2) | −66 | 166 | 55 | 76 | −155 | −70 | −161 |
| G(3) | −72 | −176 | 57 | 83 | −163 | −66 | −165 |
| T(4) | 145 | −170 | 53 | 88 | −165 | −75 | −151 |
| A(5) | −71 | 172 | 179 | 88 | −145 | −62 | −166 |
| C(6) | −62 | 167 | 52 | 78 | −149 | −70 | −159 |
| G(7) | −73 | −169 | 57 | 81 | −167 | −64 | −166 |
| 5-BrU(8) | — | — | 50 | 87 | — | — | −145 |

**Table 7**
Furanose ring conformation and parameters d[ACGTACG(5-BrU)].

| Base | Phase | Ampli | Pucker | v2 (C1′—C2′—C3′—C4′) (°) |
|---|---|---|---|---|
| A(1) | 10.6 | 38.9 | C3′-*endo* | 100 |
| C(2) | 15.6 | 48.0 | C3′-*endo* | 97 |
| G(3) | 9.1 | 44.7 | C3′-*endo* | 98 |
| T(4) | 13.4 | 41.1 | C3′-*endo* | 98 |
| A(5) | 358.2 | 40.9 | C2′-*exo*/C3′-*endo* | 97 |
| C(6) | 10.1 | 47.8 | C3′-*endo* | 98 |
| G(7) | 15.1 | 41.8 | C3′-*endo* | 100 |
| 5-BrU(8) | 18.8 | 40.0 | C3′-*endo* | 100 |

**Table 8**
Base-pair parameters for d[ACGTACG(5-BrU)].

| Base pair | *x* disp (Å) | Inclin (°) | Tip (°) | Buckle (°) | Propeller twist (°) |
|---|---|---|---|---|---|
| A(1)–5BrU(16) | −4.7 | 9.5 | 0.3 | 1.8 | −14.4 |
| C(2)–G(15) | −4.1 | 9.3 | −2.8 | 7.8 | −16.4 |
| G(3)–C(14) | −4.3 | 8.7 | 2.4 | −4.6 | −15.4 |
| T(4)–A(13) | −4.4 | 9.2 | −1.5 | −4.8 | −9.1 |

## 3. Results and discussion

d[ACGTACG(5-BrU)] crystallizes in the tetragonal space group $P4_32_12$, $a = b = 43.597$ and $c = 26.268$ Å. A summary of the refinement parameters are shown in Table 5.

### 3.1. Crystal packing

The sequence consists of alternating purine–pyrimidine bases and therefore contains the central pyrimidine–purine step, which is thought to be prerequisite for crystallization of octamer DNA in this form (Tippin & Sundaralingam, 1996), otherwise the crystal form is predominantly influenced by crystal packing effects. The structure is an A-DNA comprising a single strand in the asymmetric unit with Watson–Crick base pairing to a complementary strand. The two strands are related *via* a crystallographic dyad along the unit-cell diagonal, and there are a total of four duplexes in the unit cell. The average helical twist is 32.8° with, therefore, 11 base pairs per turn and the helix axis has a total angle of curvature of 4.5° bending toward the DNA minor groove. Nucleotides are labelled A(1) to 5-BrU(8) on strand 1, the asymmetric unit, and A(9) to 5-BrU(16) on strand 2, in a 5′ to 3′ direction.

The crystal packing is similar to that encountered in other A-form DNA octamers with the same symmetry (Wang *et al.*, 1982), where the terminal base pairs of each molecule slot into the minor groove of adjacent duplexes, and the helix axis points towards the sugar–phosphate backbone. The packing motif is stabilized by extensive van der Waals interactions as well as the formation of pseudo-base triplets (Tippin & Sundaralingam, 1996). These cross-strand triplets arise from the interaction of the N3 of the acceptor base A(1) and N2 of the donor symmetry equivalent base G(3) with a hydrogen-bond distance of 3.48 Å. The same interactions were reported by Tippin & Sundaralingam (1996) for the sequences d(GTGTACAC), d(GGGCGCCC) and d(GTGCGCAC) which show equivalent interduplex purine–purine hydrogen bonding.

Values for the torsion angles of the backbone together with the conformation of the glycosyl bond ($\chi$) are presented in Table 6. The values follow the expected trends for A-DNA except for the sugar phosphate backbone at the TpA step, which is fully extended. This is evident from the anomalous torsion angles: $\alpha$ at T(4) and $\gamma$ at A(5) where T(4)$\alpha$ is *trans* instead of *gauche*$^-$ and A(5)$\gamma$ is *trans* instead of *gauche*$^+$. The extended backbone at the fifth base seems to be present throughout this family of isomorphous crystal structures (Tippin & Sundaralingam, 1996).

### 3.2. Sugar conformation

Analysis of the sugar ring conformations (Table 7) reveals that all of the ribose units are in the C3′-*endo* conformation except for residue A(5), with the unusual external torsion angle of the ribose unit, $\gamma$, which is in a C3′-*endo*/C2′-*exo* conformation.

The base-pair parameters are shown in Table 8. The *x*-displacement parameter is characteristic of A-type DNA. It shows little variation and has a large negative value. The large values for the inclination are also indicative of A-DNA.

For the base-step parameters (Table 9), the large negative slide at the pyrimidine–purine step CG/CG indicates cross-strand overlap between opposite purine bases (Calladine & Drew, 1984). Both base pairs have large, negative propeller twist and as a result the roll parameter at this step is large: 12.7°. The TA/TA step is also a pyrimidine–purine step with a high negative slide and therefore exhibits a degree of cross-strand overlapping. The value for the propeller twist is lower for these base pairs however, and, as a result, so is the roll

**Table 9**
Global and local base-step parameters for d[ACGTACG(5-BrU)].

Local parameters are shown in bold.

| Base step | Base-pair rise (Å) | | Tilt (°) | | Slide (Å) | | Roll (°) | | Twist (°) | |
|---|---|---|---|---|---|---|---|---|---|---|
| A(1)–5BrU(16) | 2.7 | **3.3** | 0.2 | **1.2** | 0.4 | **−1.8** | −0.3 | **5.4** | 34.1 | **32.7** |
| C(2)–G(15) | 3.1 | **3.7** | −0.8 | **−0.7** | −0.3 | **−2.1** | 8.1 | **12.7** | 31.6 | **31.7** |
| G(3)–C(14) | 3.2 | **3.4** | −0.3 | **−0.8** | 0.1 | **−2.1** | −5.9 | **−0.1** | 35.9 | **35.6** |
| T(4)–A(13) | 3.0 | **3.1** | 0.0 | **0.0** | 0.0 | **−1.9** | −0.0 | **4.5** | 29.9 | **29.7** |
| A(5)–T(12) | | | | | | | | | | |
| Average | 3.0 | **3.4** | 0.0 | **0.0** | 0.1 | **−2.0** | 0.5 | **5.8** | 33.3 | **32.8** |

parameter. The small value for the helical twist as a result of the extended backbone conformation at the TpA step.

### 3.3. Groove parameters

The width of the minor groove varies from 9.5 to 10.5 Å, the large value being similar to other examples of A-DNA (Stofer & Lavery, 1994). Since the crystals pack with ends of one molecule inserted into the minor groove of an adjacent molecule, the observed trend in the minor groove width may be a result of the crystal packing. Fig. 4 shows the minor-groove width of the brominated oligonucleotide and the non-brominated analogue. Although displaying an identical trend in the variation of groove width along the molecule *i.e.* wider towards the centre, the non-brominated molecule has a minor groove which is 0.5 Å narrower. As far as the calculation of the minor-groove parameter extends, it shows the expected correlation with the $x$ displacement and inclination parameters (Boutonnet *et al.*, 1993). As the groove becomes wider, so the $x$ displacement becomes more negative, ranging from −4.4 Å at the central AT base pairs, increasing to −4.1 Å at the penultimate CG base pairs. The $x$ displacement then decreases again to −4.7 Å at the terminal base pairs, however in the case of oligonucleotides, the groove can only be defined within a certain limiting distance from its ends (Stofer & Lavery, 1994). The values of the inclination show correlation with the minor groove width *i.e.* larger in the centre, then decreasing again, for as far as the groove can be defined.

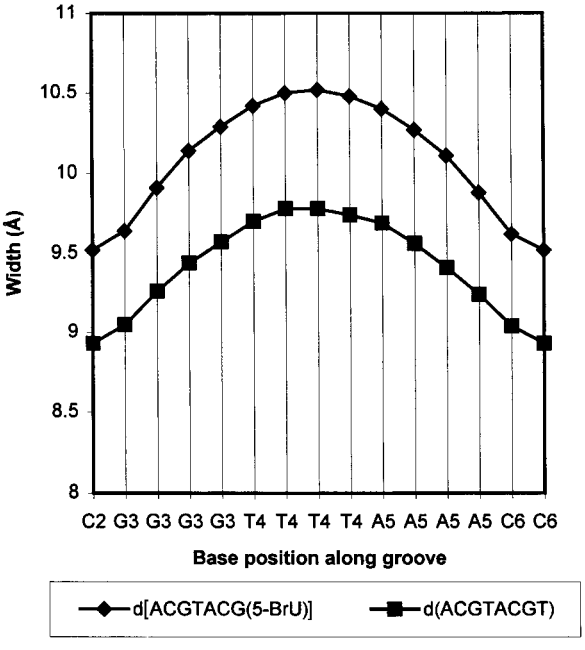


**Figure 4**
Minor-groove widths for d[ACGTACG(5-BrU)]$_2$ and d(ACGTACGT)$_2$ (Wilcock *et al.*, 1996). Both grooves were calculated with the program *CURVES*.

## 4. Conclusions

The power of MAD phasing in combination with density modification is very well illustrated in this particular example. The treatment of multiwavelength anomalous diffraction data as a special case of multiple isomorphous replacement, in contradistinction to the Hendrickson treatment available with the program *MADLSQ*, does not require the explicit determination of $f'$ and $f''$, but does require determination of the heavy-atom positions. The 'native' data set does not have to be the data set which is subsequently used for refinement. In the present work, the inflection point data set ($f''$ at its largest magnitude) was used as the native during the phasing procedure, but the highest energy data set (0.9002 Å) used as the data set for refinement, because it was measured to the highest resolution in a fixed geometry. Another strategy which would be appropriate would be to refine against the data set measured on the lower side of the absorption edge, which should result in the data set with the lowest possible correction for absorption effects. For the use of other software packages which also use the MIR approach to MAD phasing, see *e.g.*, Terwilliger (1997) and Ramakrishnan & Biou (1997). The map is of high quality, and would have enabled rapid model building in the case that a suitable model were not available. Studies using the same methodology on unknown packings obtained from the binding of antitumour agents to sequences such as this have now succeeded, as mentioned above.

DNA octanucleotides crystallize in the A form in the solid state, although they adopt the B form in solution (Clark *et al.*, 1990), which is ascribed to the favourable packing adopted by A-form octamers (Neidle, 1994). The asymmetric unit is a single octamer chain with 96 associated water molecules. There is a measured volume increase compared with the native octamer measured at room temperature of 9.6%. The bromine substitution is at the end of the sequence, so it is particularly favourable position for isomorphism. Comparison of the native and brominated octamers shows that both the minor-groove width and the overall molecular diameter are somewhat increased by bromination. The increase in groove width of about 0.5 Å has already been discussed. The molecular diameter, as measured by the P–P separation ranges from 18.73 to 19.47 Å in the native, and from 19.07 to 20.13 Å in the brominated analogue. These increases are greater than those in the lattice constants, but all may be due to a higher

degree of hydration caused by bromination, and due to the more highly polar nature of the Br atom compared with that of the methyl group, isosteric though they may be.

If brominated oligonucleotides are to be treated as more than just heavy-atom derivatives, it is important to be aware of these subtle differences.

We thank the Association for International Cancer Research for a Fellowship (to AA), the BBSRC for a Studentship (to ART), the European Union for financial support (to DJW). Professor Keith Tipton kindly provided the laboratory space in Trinity College for AA. Dr S. J. Salisbury (Cambridge Crystallographic Data Centre), Dr P. R. Evans (MRC Laboratory of Molecular Biology, Cambridge) and Dr E. Dodson (University of York) are thanked for helpful discussions.

## References

Baikalov, I. & Dickerson, R. E. (1998). *Acta Cryst.* D**54**, 324–333.
Boutonnet, N., Hui, X. & Zakrzewska, K. (1993). *Biopolymers*, **33**, 479–490.
Calladine, C. R. & Drew, H. R. (1984). *J. Mol. Biol.* **178**, 773–781.
Clark, G. R., Brown, D. G., Sanderson, M. R., Chwalinski, T., Neidle, S., Veal, J. M., Jones, R. L., Wilson, W. D., Garman, E. & Stuart, D. I. (1990). *Nucleic Acids Res.* **18**, 5521–5528.
Clowney, L., Jain, S. C., Srinivasan, A. R., Westbrook, J., Olson, W. K. & Berman, H. M. (1996). *J. Am. Chem. Soc.* **118**, 509–518.
Collaborative Computational Project, Number 4 (1994). *Acta Cryst.* D**50**, 760–763.
Crane, B. R., Bellamy, H. & Getzoff, E. D. (1997). *Acta Cryst.* D**53**, 8–22.
Gelbin, A., Schneider, B., Clowney, L., Hsieh, S.-H., Olson, W. K. & Berman, H. M. (1996). *J. Am. Chem. Soc.* **118**, 519–529.
Hendrickson, W. (1991). *Science*, **25**, 51–58.
Hendrickson, W. A. & Ogata, C. M. (1997). *Methods Enzymol.* **276**, 494–523.
Jones, T. A., Zou, J. Y., Cowan, S. W. & Kjeldgaard, M. (1991). *Acta Cryst.* A**47**, 110–119.
Lavery, R. & Sklenar, H. (1989). *J. Biomol. Struct. Dynam.* **6**, 655–667.
Neidle, S. (1994). *DNA Structure and Recognition*. Oxford: IRL Press.
Otwinowski, Z. (1993). *Data Collection and Processing*, *Proceedings of the Daresbury Study Weekend*, edited by L. Sawyer, N. Isaacs & S. Bailey, Warrington: Daresbury Laboratory.
Peterson, M. R., Harrop, S. J., McSweeney, S. M., Leonard, G. A., Thompson, A. W., Hunter, W. N. & Helliwell, J. R. (1996). *J. Synchrotron Rad.* **3**, 24–34.
Powell, H. R. (1997). *MAD-DM at Elettra; a Case Study. Proceedings of the CCP4 Study Weekend*, edited by S. Bailey, K. Wilson & G. Davies. Warrington: Daresbury Laboratory.
Ramakrishnan, V. & Biou, V. (1997). *Methods Enzymol.* **276**, 538–557.
Sheldrick, G. & Gould, R. O. (1995). *Acta Cryst.* B**51**, 423–431.
Smith, J. (1997). *New Advances in Phasing*, *Proceedings of the CCP4 Study Weekend*, edited by S. Bailey, K. Wilson & G. Davies. Warrington: Daresbury Laboratory.
Stofer, E. & Lavery, R. (1994). *Biopolymers*, **34**, 337–346.
Terwilliger, T. C. (1997). *Methods Enzymol.* **276**, 530–537.
Tippin, D. B. & Sundaralingam, M. (1996). *Acta Cryst.* D**52**, 997–1003.
Todd, A. R., Adams, A., Thorpe, J. M., Denny, W. J., Wakelin, L. P. G. & Cardin, C. J. (1999). In the press.
Wang, A. J.-H., Fujii, S., van Boom, J. H. & Rich, A. (1982). *Proc. Natl Acad. Sci. USA*, **79**, 3968–3972.
Wilcock, D. J., Adams, A., Cardin, C. J. & Wakelin, L. P. G. (1996). *Acta Cryst.* D**52**, 481–485.